

Substituent Effects in Five Oxo-Centered Trinuclear Rhodium(III) Clusters

Jacqueline R. Houston,[†] Marilyn M. Olmstead,[†] and William H. Casey^{*†‡}

Departments of Chemistry and Geology, University of California, Davis, Davis, California 95616

Received May 15, 2006

We here report the rates of water substitution by methanol-*d*₄ for four new oxo-centered trinuclear rhodium(III) clusters with different carboxylate-bridging ligands, [Rh₃(μ₃-O)(μ-O₂CR)₆(OH₂)₃]⁺ (R = CH₂CH₃, CH₂CH₂Cl, CH₂Cl, and CHCl₂), and [Rh₃(μ₃-O)(μ-O₂CCH₃)₆(OH₂)₃]⁺. By varying the R group alkyl chain, water substitution rates were found to span almost 3 orders of magnitude ($k^{298K} = 1.2 \times 10^{-2}$ – 2.3×10^{-5} s⁻¹) and reflect the following trend R = CH₂CH₃ > CH₃ > CH₂CH₂Cl > CH₂Cl > CHCl₂. Activation parameters for substitution point toward a dissociative activation pathway ($\Delta H^\ddagger = 99$ – 115 kJ mol⁻¹; $\Delta S^\ddagger = 48$ – 52 J mol⁻¹ K⁻¹), indicating that there is little association with the incoming methanol molecule during the formation of the transition-state complex. Because the mechanism for substitution in all five trimers has a considerable dissociative character, substitution rates are likely very similar to water exchange rates. These data suggest that the kinetic reactivity of the ligated waters is heavily influenced by the inductive ability of the aliphatic substituents, but yet the mechanism of substitution remains virtually unchanged. Structural data are also reported for the four new rhodium(III) trimer salts as well as ¹⁰³Rh NMR spectra. We find that ¹⁰³Rh NMR chemical shifts span more than 200 ppm and mirror the same reactivity trend found for the rates of water substitution (¹⁰³Rh δ (9406–9620 ppm): R = CH₂CH₃ < CH₃ < CH₂CH₂Cl < CH₂Cl < CHCl₂). Taken together, these data suggest a means for estimating water exchange rates for other oxo-centered rhodium(III) trimers from chemical shift data alone.

Introduction

Recent work has uncovered counterintuitive chemistry for ligand substitutions in inert metal complexes.^{1–3} For example, because the hexa-aqua-rhodium(III) ion is a low-spin octahedral metal with saturated t_{2g}⁶ orbitals, water exchange from [Rh(OH₂)₆]³⁺ is expected to undergo a dissociative-like activation pathway because the approach of a seventh ligand would be electrostatically disfavored. However, based on the negative activation volume ($\Delta V^\ddagger = -4.2$ cm³ mol⁻¹) and quantum calculations,^{4,5} an interchange-associative (I_a) mechanism is clear.

This ion reacts atypically among the other rhodium(III) complexes, for which dissociative activation pathways for water exchange have been found. To name a few, water exchanges from [Rh(OH₂)₅OH]²⁺,¹ [Cp*Rh(OH₂)₃]²⁺,⁶ [Rh(CH₃NH₂)₅H₂O]³⁺,⁷ [(H₂O)₄Rh(μ-OH)₂Rh(OH₂)₄]⁴⁺,⁸ and [Rh₃(μ₃-O)(μ-O₂CCH₃)₆(OH₂)₃]⁺⁹ all follow a dissociative (D) or interchange-dissociative (I_d) mechanism based on highly positive activation parameters. Rates of water exchange are also significantly faster than that of [Rh(OH₂)₆]³⁺, by approximately 2–6 orders of magnitude. This enhanced kinetic reactivity results from electron donation from the other coordinated ligands, which labilizes the bound waters (η-OH₂) to substitution and promotes a reaction mechanism that takes on a more dissociative activation state.

* To whom correspondence should be addressed. E-mail: whcasey@ucdavis.edu.

[†] Department of Chemistry.

[‡] Department of Geology.

- (1) Laurency, G.; Rapaport, I.; Zbinden, D.; Merbach, A. E. *Magn. Reson. Chem.* **1991**, *29* (special issue), S45–S51.
- (2) Galbraith, S. C.; Robson, C. R.; Richens, D. T. *J. Chem. Soc., Dalton Trans.* **2002**, *23*, 4335–4338.
- (3) Cusanelli, A.; Frey, U.; Richens, D. T.; Merbach, A. E. *J. Am. Chem. Soc.* **1996**, *118*, 5265–5271.
- (4) De Vito, D.; Sidorenkova, H.; Rotzinger, F. P.; Weber, J.; Merbach, A. E. *Inorg. Chem.* **2000**, *39*, 5547–5552.

- (5) De Vito, D.; Weber, J.; Merbach, A. E. *Inorg. Chem.* **2004**, *43*, 858–864.

- (6) Dadci, L.; Elias, H.; Frey, U.; Hoernig, A.; Koelle, U.; Merbach, A. E.; Paulus, H.; Schneider, J. S. *Inorg. Chem.* **1995**, *34*, 306–315.

- (7) Gonzalez, G.; Moullet, B.; Martinez, M.; Merbach, A. E. *Inorg. Chem.* **1994**, *33*, 2330–2333.

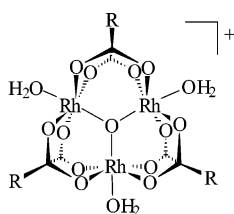
- (8) Drljaca, A.; Zahl, A.; van Eldik, R. *Inorg. Chem.* **1998**, *37*, 3948–3953.

- (9) Houston, J. R.; Yu, P.; Casey, W. H. *Inorg. Chem.* **2005**, *44*, 5176–5182.

Table 1. Crystallographic Data for Rh_3^+ ($\text{R} = \text{CH}_2\text{CH}_3, \text{CH}_2\text{Cl}, \text{CHCl}_2, \text{and } \text{CH}_2\text{CH}_2\text{Cl}$) Perchlorate Salts

compound	$\text{R} = \text{CH}_2\text{CH}_3$	$\text{R} = \text{CH}_2\text{Cl}, 9\text{H}_2\text{O}$	$\text{R} = \text{CHCl}_2, 2\text{H}_2\text{O}$	$\text{R} = \text{CH}_2\text{CH}_2\text{Cl}, 0.5\text{H}_2\text{O}$
formula	$\text{C}_{18}\text{H}_{36}\text{ClO}_{20}\text{Rh}_3$	$\text{C}_{12}\text{H}_{36}\text{Cl}_7\text{O}_{29}\text{Rh}_3$	$\text{C}_{12}\text{H}_{16}\text{Cl}_{13}\text{O}_{22}\text{Rh}_3$	$\text{C}_{18}\text{H}_{31}\text{Cl}_7\text{O}_{20.5}\text{Rh}_3$
formula weight	916.64	1201.29	1281.83	1132.31
cryst syst	trigonal	trigonal	monoclinic	monoclinic
space group	$R\bar{3}$ (No. 148)	$R\bar{3}$ (No. 146)	Cc (No. 9)	$P2_1/n$ (No. 14)
$a, \text{\AA}$	12.6662(10)	17.9749(5)	9.9730(3)	12.1180(9)
$b, \text{\AA}$	12.6662(10)	17.9749(5)	17.3348(5)	12.6539(9)
$c, \text{\AA}$	32.509(4)	9.8130(6)	20.9982(7)	24.035(2)
α, deg	90	90	90	90
β, deg	90	90	102.78(3)	93.823(2)
γ, deg	120	120	90	90
$V, \text{\AA}^3$	4516.7(7)	2745.8(2)	3540.3(2)	3677.3(5)
Z	6	3	4	4
$T, ^\circ\text{C}$	-183(2)	-183(2)	-178(2)	-180(2)
$\lambda, \text{\AA}$	0.710 73	0.710 73	0.710 73	0.710 73
$D_{\text{calcd}}, \text{g cm}^{-3}$	2.022	2.179	2.405	2.405
μ, mm^{-1}	1.797	1.947	2.446	1.915
$R1 [I > 2\sigma(I)]$	0.0157	0.0130	0.0160	0.0452
wR2 (all data)	0.0393	0.0327	0.0396	0.1272

To understand how these inductive effects from neighboring ligands influence the reaction rates, we examine a series of oxo-centered rhodium(III) trimers with different carboxylate-bridging ligands, $[\text{Rh}_3(\mu_3\text{-O})(\mu\text{-O}_2\text{CR})_6(\text{OH}_2)_3]^+$ ($\text{R} = \text{aliphatic substituent}$). In these complexes, the three $\eta\text{-OH}_2$ are located cis from the bridging carboxylates ($\mu\text{-O}_2\text{CR}$) and can be more than 6 orders of magnitude more reactive than the $\eta\text{-OH}_2$ on the hexa-aquarhodium(III) ion $[\text{Rh}_3(\mu_3\text{-O})(\mu\text{-O}_2\text{CCH}_3)_6(\text{OH}_2)_3]^+$, $k_{\text{ex}}^{298\text{K}} = 5 \times 10^{-3} \text{ s}^{-1}$; $[\text{Rh}(\text{OH}_2)_6]^{3+}$, $k_{\text{ex}}^{298\text{K}} = 2.2 \times 10^{-9} \text{ s}^{-1}$.^{1,9} As was already suggested for oxo-centered chromium(III) trimers,¹⁰ combined inductive effects from the $\mu\text{-O}_2\text{CCH}_3$ and $\mu_3\text{-O}$ are likely responsible for this $\sim 10^6$ -fold labilization among these rhodium(III) ions. To separate these two effects, we examined water substitution from four new oxo-centered rhodium(III) trimers, $[\text{Rh}_3(\mu_3\text{-O})(\mu\text{-O}_2\text{CR})_6(\text{OH}_2)_3]^+$ ($\text{R} = \text{CH}_2\text{CH}_3, \text{CH}_2\text{Cl}, \text{CHCl}_2, \text{and } \text{CH}_2\text{CH}_2\text{Cl}$; abbreviated as Rh_3^+ in the subsequent text), and $[\text{Rh}_3(\mu_3\text{-O})(\mu\text{-O}_2\text{CCH}_3)_6(\text{OH}_2)_3]^+$ and speculate based on activation parameters the mechanism of substitution at each of these molecules.



$\text{R} = \text{CH}_3, \text{CH}_2\text{CH}_3, \text{CH}_2\text{CH}_2\text{Cl}, \text{CH}_2\text{Cl}, \text{CHCl}_2$

Materials and Methods

Syntheses. All Rh_3^+ cations were synthesized by heating 300–500 mg of the rhodium active-hydroxide solid, $\text{Rh}(\text{OH})_3 \cdot x\text{H}_2\text{O}$,^{11,12} dissolved in the corresponding carboxylic acid (>3 mol equiv in 5 mL of water) at 333 K for 24 h. The purification and crystallization procedure was the same as that discussed by Houston et al. in ref 9. Typical yields, determined by weight, were 60–45% for Rh_3^+ with $\text{R} = \text{CH}_2\text{CH}_3, \text{CH}_2\text{Cl}, \text{and } \text{CHCl}_2$ but low ($\sim 10\%$) for $\text{R} = \text{CH}_2\text{CH}_2\text{Cl}$. The synthesis using 3-chloropropionic acid produced a brown-green solution after heating for longer than 6 h, from which green-blue crystals deposited after several days of slow evaporation. The identity of these crystals was confirmed to be the 3-chloropropionate-bridged rhodium(II) dimer (see the CIF file in the

Supporting Information) and therefore accounts for the low product yield of the oxo-centered rhodium(III) trimer. The purity of all stock crystals was ensured by measuring the ^1H NMR spectrum (see Figure S1 in the Supporting Information). Elem anal. Found (calcd for Rh_3^+ with $\text{R} = \text{CH}_2\text{Cl}, 9\text{H}_2\text{O}$): C, 12.72 (12.00); H, 2.66 (3.02); Rh, 25.5 (25.7). Found (calcd for Rh_3^+ with $\text{R} = \text{CH}_2\text{CH}_2\text{Cl}, 0.5\text{H}_2\text{O}, 2\text{NaClO}_4$; residual sodium perchlorate crystals were present in the Rh_3^+ ($\text{R} = \text{CH}_2\text{CH}_2\text{Cl}$) sample from the crystallization process): C, 15.80 (15.70); H, 2.59 (2.27); Rh, 22.9 (22.4). Found (calcd for Rh_3^+ with $\text{R} = \text{CHCl}_2, 2\text{H}_2\text{O}$): C, 11.22 (11.24); H, 1.26 (1.26); Rh, 23.2 (24.1). Found (calcd for Rh_3^+ with $\text{R} = \text{CH}_3, 2\text{H}_2\text{O}$): C, 16.35 (16.59); H, 3.26 (3.25); Rh, 32.6 (35.5). Found (calcd for Rh_3^+ with $\text{R} = \text{CH}_2\text{CH}_3$): C, 23.56 (23.58); H, 3.95 (3.96); Rh, 31.4 (33.6). All C/Rh molar ratios correspond to the expected stoichiometry from X-ray crystallography data. For Rh_3^+ ($\text{R} = \text{CH}_2\text{CH}_2\text{Cl}$), not all sodium perchlorate crystals; could be physically separated from the rhodium(III) crystals, the formula mass was adjusted to account for 2 mol of NaClO_4 . Regardless of whether the adjustment was made, the C/Rh molar ratio from the microanalysis still gave the expected stoichiometry (C:Rh = 6:1) based on the molecular formula obtained from crystallography data [C:Rh = 18.11:3.06 (anal.) for $\text{C}_{18}\text{H}_{31}\text{Cl}_7\text{O}_{20.5}\text{Rh}_3$ (see the X-ray Crystallography section)].

X-ray Crystallography. Selected crystals were mounted in a N_2 cold stream provided by a Cryo Industries apparatus on the goniometer of a Bruker SMART 1000 CCD based diffractometer. Data were collected with the use of Mo $K\alpha$ radiation. No decay in the intensities of equivalent reflections was noted. Corrections for absorption were carried out using a multiscan technique.¹³ The structures were solved by direct methods and difference Fourier techniques and refined using the *SHELXTL 5.1* package.¹⁴ Crystal data and experimental details are summarized in Table 1. Additional details are available in the Supporting Information as CIF files.

^{103}Rh NMR Spectroscopy. Perchlorate crystals were dissolved in 0.01 M HClO_4 [solution pH = 1.9–2.1 (± 0.1)] to ensure that the complexes were in their fully protonated form $[\text{Rh}_3^+$ ($\text{R} = \text{CH}_3$); $\text{p}K_{\text{a}} = 8.3$ (± 0.2)]. Because the solubility of Rh_3^+ ($\text{R} = \text{CH}_2\text{Cl}, \text{CHCl}_2, \text{and } \text{CH}_2\text{CH}_2\text{Cl}$) in water at 298 K was relatively low, all

- (10) Fujihara, T.; Aonahata, J.; Kumakura, S.; Nagasawa, A.; Murakami, K.; Ito, T. *Inorg. Chem.* **1998**, *37*, 3779–3784.
- (11) Ayres, H. R.; Forrester, J. S. *J. Inorg. Chem.* **1957**, *3*, 365–366.
- (12) Crimp, S. J.; Spiccia, L. *Aust. J. Chem.* **1995**, *48*, 557–566.
- (13) Sheldrick, G. M. *SADABS*, version 2.10; University of Göttingen: Göttingen, Germany, 2003.
- (14) Sheldrick, G. M. *SHELXTL*, version 5.1; Siemens Analytical X-ray Instruments: Madison, WI, 1998.

^{103}Rh NMR spectra were acquired at 338.7 K (± 0.5 K) so that ^{103}Rh NMR chemical shifts would be comparable. The sample concentration of Rh_3^+ varied from 0.02 to 0.1 M because even at 338.7 K the solubility of Rh_3^+ with $\text{R} = \text{CH}_2\text{Cl}$ and CHCl_2 was still less than 0.05 M. Organic solvents that could improve the solubility of the complexes were avoided because of substitution of $\eta\text{-OH}_2$. Each Rh_3^+ sample was placed in a 10-mm NMR tube containing a coaxial insert of 0.5 M $\text{Rh}(\text{H}_2\text{O})_6^{3+}$ dissolved in $\text{D}_2\text{O}/\text{HClO}_4$ (3:1, $\text{pH} < 0$). The $\text{Rh}(\text{H}_2\text{O})_6^{3+}/\text{D}_2\text{O}$ solution provided a chemical shift reference ($\delta = 9915.8$ ppm at 298 K; $\delta = 9994.4$ ppm at 338.7 K) and an external lock signal.^{9,15}

The ^{103}Rh NMR spectra were acquired on a Bruker Avance spectrometer (11.7 T; $\nu_0 = 15.9$ MHz) via direct observation using a 10-mm broad-band probe. Because of the insensitivity of the ^{103}Rh nucleus, the $\pi/2$ pulse was not determined, so a conservative pulse width of 15 μs was used to avoid signal saturation, consistent with previously published work.⁹ Depending on the $[\text{Rh}_3^+]$, 7000–50 000 scans were obtained over a spectral width of 28.7 kHz using a pulse-repetition time of 1.5 s.

^1H NMR Kinetic Experiments. Perchlorate crystals of the rhodium(III) compound were dissolved in thermally equilibrated CD_3OD (600 μL acidified with 10 μL of 1 M HClO_4) to give a $[\text{Rh}_3^+] = 12$ mM solution. After dissolution, the sample was immediately transferred to the NMR spectrometer, which took no longer than 5 min.

The ^1H NMR spectra were acquired at $\nu_0 = 500.1$ MHz (11.7 T field) using a 5-mm probe. A 3- μs pulse was used (35° tip, $\pi/2 = 7.6$ μs) with a delay of 1 s over a spectral region of 6 kHz. A total of eight scans was collected. For those Rh_3^+ complexes in which scalar coupling between adjacent protons occurs (i.e., $\text{R} = \text{CH}_2\text{-CH}_3$), homonuclear decoupling was performed to collapse the multiplets so that ^1H signals due to all CD_3OD -substituted Rh_3^+ species could be resolved within the region. All ^1H NMR chemical shifts are reported relative to tetramethylsilane.

The rates of water substitution by methanol- d_4 were determined by monitoring the disappearance of the ^1H NMR signal due to the $\mu\text{-O}_2\text{CR}$ protons of the triaqua trimer as a function of time (see ref 16). Because there are three $\eta\text{-OH}_2$ sites, multiple substitutions by methanol are possible. These sites give rise to several signals on the ^1H NMR spectrum, but these peaks are relatively well resolved from the signal due to the triaqua trimer. Even though the peaks were relatively well resolved, peak intensities were obtained from a least-squares fit of the frequency-domain data to a sum of Lorentzian curves using a line-fitting program. Peak heights were fit to the following three-parameter exponential equation in order to extract rate coefficients (eq 1). The terms I_∞ and I_t refer to the

$$I_t = I_\infty + ae^{-kt} \quad (1)$$

peak height at time equal to infinity and the normalized peak height of the ^1H NMR signal during the course of the experiment, respectively. The term I_∞ is an adjustable parameter used to approximate the equilibrium concentration of the triaqua trimer in solution and did not deviate much from zero. The term k refers to the rate coefficient for water substitution by methanol- d_4 , a is an adjustable parameter, and t is the elapsed time from mixing.

Activation parameters [enthalpy (ΔH^\ddagger) and entropy (ΔS^\ddagger)] were calculated from the temperature dependence of the rate using the Eyring equation (eq 2). The term k represents the rate coefficient

$$k = \frac{k_B T}{h} e^{-[(\Delta H^\ddagger - T\Delta S^\ddagger)/RT]} \quad (2)$$

for substitution, k_B is the Boltzmann constant, T is the experimental temperature in Kelvin, h is Planck's constant, and R is the gas constant.¹⁷

Because the Rh_3^+ ($\text{R} = \text{CH}_2\text{CH}_3$ and CH_3) ions are so reactive, only low temperatures could be used for the variable-temperature experiments. However, to ensure that the ^1H signals due to each trimeric molecule were resolvable, temperatures lower than 266 K were avoided to prevent significant line broadening. All sample temperatures were determined with a copper–constantan thermocouple placed inside a separate NMR tube but with similar geometry and sample composition. We estimate the error in the temperature readings to be less than ± 0.5 K.

Results

Crystal Structures. A considerable number of oxo-centered carboxylate-bridged trimers of formula $[\text{M}_3(\mu_3\text{-O})(\mu\text{-O}_2\text{CR})_6\text{L}_3]^{n+}$ are known, in particular, those of trivalent Cr, Mn, Fe, and Ru cations as well as mixed-valent species that give rise to neutral complexes.^{18–27} Surprisingly, there are just a few reports of trivalent Co and Rh salts.^{28–30} In the case of rhodium(III), only two polymorphs of the perchlorate salt of Rh_3^+ ($\text{R} = \text{CH}_3$) have been reported,³⁰ one a dihydrate (A) and the other a monohydrate (B). In view of the paucity of information and in order to assess the possible influence of these data on water substitution rates, a comparison of these structures is made.

Figure 1 shows a packing diagram for the structure of Rh_3^+ ($\text{R} = \text{CH}_2\text{CH}_3$), and thermal ellipsoid drawings for all structures are provided in the Supporting Information. In all of the compounds, the central trimeric core is essentially planar, in which each rhodium(III) ion is in an octahedral coordination environment. The Rh-O-Rh angles range from 119° to 120° , and the $\text{Rh}\cdots\text{Rh}$ distances are in the range 3.317–3.358 Å, which is outside normal metal–metal

- (15) Read, M. C.; Glaser, J.; Sandström, M.; Toth, I. *Inorg. Chem.* **1992**, *31*, 4155–4159.
- (16) Sasaki, Y.; Nagasawa, A.; Tokiwa-Yamanoto, A.; Ito, T. *Inorg. Chim. Acta* **1993**, *212*, 175–182.
- (17) Wilkins, R. G. *Kinetics and Mechanism of Reactions of Transition Metal Complexes*, 2nd ed.; VCH: Weinheim, Germany, 1991.
- (18) Oh, S. M.; Henderickson, D. N.; Hassett, K. L.; Davis, R. E. *J. Am. Chem. Soc.* **1985**, *107*, 8009–8018.
- (19) Harton, A.; Nagi, M. K.; Glass, M. M.; Junk, P. C.; Atwood, J. L.; Vincent, J. B. *Inorg. Chim. Acta* **1994**, *217*, 171–179.
- (20) Baikie, A. R. E.; Hursthouse, M. B.; New, D. B.; Thornton, P. J. *Chem. Soc., Chem. Commun.* **1978**, *2*, 62–63.
- (21) Bond, A. M.; Clark, R. J. H.; Humphrey, D. G.; Panayiotopoulos, P.; Skelton, B. W.; White, A. H. *J. Chem. Soc., Dalton Trans.* **1998**, *11*, 1845–1852.
- (22) Cotton, F. A.; Norman, J. G.; Spencer, A.; Wilkinson, G. *J. Chem. Soc., Chem. Commun., Sect. D* **1971**, *16*, 967–968.
- (23) Cotton, F. A.; Norman, J. G., Jr. *Inorg. Chim. Acta* **1972**, *6*, 411–419.
- (24) Spencer, A.; Wilkinson, G. *J. Chem. Soc., Dalton Trans.* **1972**, *14*, 1570–1577.
- (25) Chang, S.; Jeffrey, G. A. *Acta Crystallogr., Sect. B* **1970**, *26*, 673–683.
- (26) Anzenhofer, K.; De Boer, J. J. *Recl. Trav. Chim. Pays-Bas* **1969**, *88*, 286–288.
- (27) Blake, A. B.; Fraser, L. R. *J. Chem. Soc., Dalton Trans.* **1975**, *3*, 193–197.
- (28) Beattie, J. K.; Hambley, T. W.; Klepetko, J. A.; Masters, A. F.; Turner, P. *Polyhedron* **1996**, *15*, 2141–2150.
- (29) Abe, M.; Sasaki, Y.; Yamada, Y.; Tsukahara, K.; Yano, S.; Ito, T. *Inorg. Chem.* **1995**, *34*, 4490–4498.
- (30) Glowiak, T.; Kubiak, M.; Szymanska-Buzar, T. *Acta Crystallogr., Sect. B* **1977**, *B33*, 1732–1737.

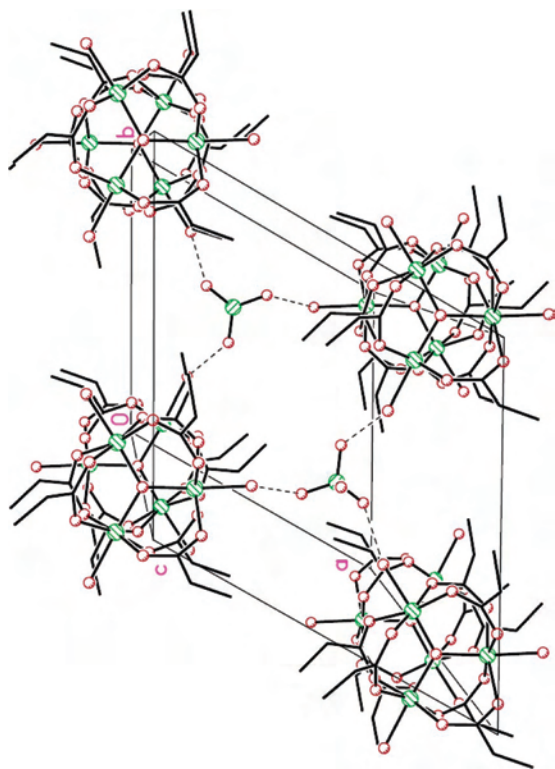


Figure 1. Unit cell for $[\text{Rh}_3(\mu_3\text{-O})(\mu\text{-O}_2\text{CCH}_2\text{CH}_3)_6(\text{OH}_2)_3]\text{ClO}_4$. The red atoms refer to oxygen ions, and the green atoms represent rhodium(III) ions and chloride in the perchlorate counterions.

bonding ranges. Select structural data for all new compounds, together with those from Rh_3^+ ($\text{R} = \text{CH}_3$), are summarized in Table 2. Among the structures being reported, only compounds Rh_3^+ with $\text{R} = \text{CH}_2\text{CH}_3$ and CH_2Cl take advantage of 3-fold crystallographic symmetry. Nevertheless, all five complexes show highly symmetrical pseudo- D_{3h} symmetry, with their primary differences residing in conformational changes in the R group alkyl chains. Also shown in Table 2 are the $\text{Rh}-\text{OH}_2$ bond lengths for the new trimers, which are all markedly shorter (2.08–2.09 Å) than those for Rh_3^+ with $\text{R} = \text{CH}_3$ (2.12 Å) reported by Glowiak et al.³⁰ As expected, $\text{Rh}-\text{O}$ bond distances increase according to the trend $\text{Rh}-\text{O}(\mu_3\text{-O}) < \text{Rh}-\text{O}(\mu\text{-O}_2\text{CR}) < \text{Rh}-\text{OH}_2$.

^{103}Rh NMR Spectra. As expected, only one ^{103}Rh NMR signal is observed for each of the oxo-centered trimers because of their idealized D_{3h} symmetry (Figure 2).⁹ The chemical shifts span more than 200 ppm (9406–9620 ppm; $T = 338.7$ K) and are comparable to those reported by Spiccia et al. for other aqueous rhodium(III) trimers.³¹ While this span is only a small fraction of the total chemical shift range for ^{103}Rh (~12 000 ppm),³² these differences in chemical shifts can be used to discriminate different electronic environments surrounding the ^{103}Rh nuclei in each trimeric moiety. On the basis of the chemical shifts, the ^{103}Rh shielding decreases in the order $\text{R} = \text{CH}_2\text{CH}_3 > \text{CH}_3 > \text{CH}_2\text{CH}_2\text{Cl} > \text{CH}_2\text{Cl} > \text{CHCl}_2$, which agrees with the

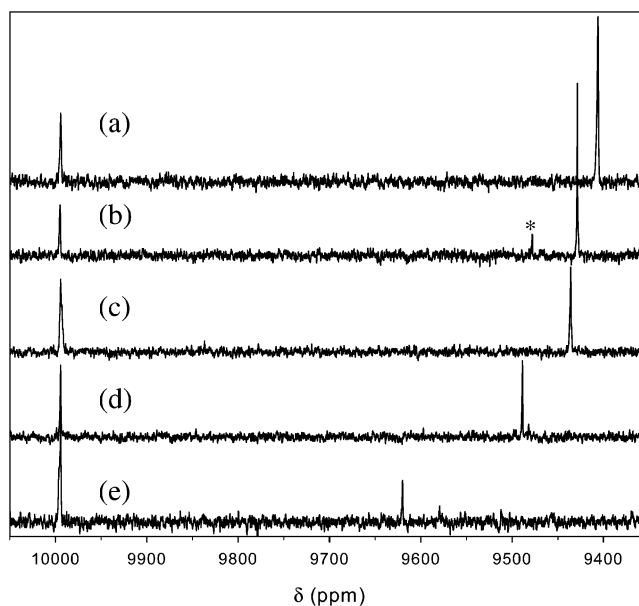


Figure 2. ^{103}Rh NMR spectra of Rh_3^+ in 0.01 M HClO_4 ($[\text{Rh}_3^+] = 0.02\text{--}0.1$ M, solution $\text{pH} = 1.9\text{--}2.2$ (± 0.1)). Spectra are as follows: $\text{R} = \text{CH}_2\text{CH}_3$ (a), CH_3 (b), $\text{CH}_2\text{CH}_2\text{Cl}$ (c), CH_2Cl (d), and CHCl_2 (e). NMR spectra were acquired using 7000–50 000 scans at 338.7 K. Note that the small peak marked with an asterisk in (b) is an impurity. All chemical shifts are reported relative to 0.5 M $\text{Rh}(\text{H}_2\text{O})_6^{3+}$ ($\text{D}_2\text{O}:\text{HClO}_4 = 3:1$, $\text{pH} < 0$) set at $\delta = 9994.4$ ppm (relative to $\delta^{298\text{K}} = 9915.8$ ppm, ref 20).

magnetochemical series proposed by Juranić³³ for d_6 transition-metal complexes and also reflects the inductive ability of the aliphatic substituents.³⁴

Water Substitution Rates. Shown in Figure 3 are ^1H NMR spectra for water substitution from Rh_3^+ ($\text{R} = \text{CHCl}_2$) at $T = 313.5$ K. Immediately after the rhodium(III) trimer is dissolved in the deuterated solvent, a large signal at 6.475 ppm is observed as a result of the protons on the $\mu\text{-O}_2\text{-CCHCl}_2$ bridges of the triqua form of the trimer. As the substitution of water by methanol- d_4 takes place, two additional peaks are observed on the spectrum (6.480 and 6.527 ppm) and indicate the presence of the monosubstituted methanol- d_4 trimer. These two peaks are in a 1:2 ratio because the three rhodium(III) ions that make up the trimeric moiety are no longer chemically equivalent. After several hours of reaction time, two more peaks appear in a 2:1 ratio as a result of the disubstituted methanol- d_4 trimer (6.534 and 6.590 ppm). After further reaction, a sixth peak appears at 6.602 ppm as a result of the trisubstituted methanol- d_4 trimer. Similar ^1H NMR spectra are observed for all other Rh_3^+ ions except that the chemical shift dispersion of the ^1H NMR signals is much smaller than that for Rh_3^+ ($\text{R} = \text{CHCl}_2$). Peak assignments for Rh_3^+ ($\text{R} = \text{CH}_3$) were previously reported by Sasaki et al., who also reported a rate for water substitution for this molecule ($k^{298\text{K}} = 1.3 \times 10^{-3} \text{ s}^{-1}$ per metal ion) and a mixed rhodium(III)/ruthenium(III) trimer.¹⁶

To determine rate constants for water substitution, the decrease in the signal height due to the triqua form of the trimer was monitored as a function of time. (Rate constants

(31) Spiccia, L.; Aramini, J. M.; Crimp, S. J.; Drljaca, A.; Lawrenz, E. T.; Tedesco, V.; Vogel, H. J. *J. Chem. Soc., Dalton Trans.* **1997**, 23, 4603–4610.

(32) Ernsting, J. M.; Gaemers, S.; Elsevier, C. J. *Magn. Reson. Chem.* **2004**, 42, 721–736.

(33) Juranić, N. *Coord. Chem. Rev.* **1989**, 96, 253–290.

(34) Taft, R. W., Jr. *Steric Effects in Organic Chemistry*; Newman, M. S., Ed.; Wiley: New York, 1956; Chapter 3.

Table 2. Select Bond Distances (Å) and Angles (deg) for the Four New Rh_3^+ Perchlorate Salts and Rh_3^+ ($\text{R} = \text{CH}_3$)^a

Rh_3^+ ($\text{R} =$)	Rh–O(H_2O)	Rh–O($\mu_3\text{-O}$)	Rh–O($\mu_2\text{-O}_2\text{CR}$)	Rh···Rh	O($\mu_3\text{-O}$)–Rh– O(H_2O)	O(H_2O)–Rh– O($\mu_2\text{-O}_2\text{CR}$)	O($\mu_3\text{-O}$)–Rh– O($\mu_2\text{-O}_2\text{CR}$)
CH_3^b A	2.129(8)	1.924(12)	2.020(12)	3.332(11)	177.5(8)	85.3(12)	94.7(5)
CH_3^b B	2.10(4)	1.92(2)	2.03(2)	3.329(3)	177.8(10)	84.8(13)	95(2)
CH_2CH_3	2.0934(9)	1.9244(2)	2.016(11)	3.3168(3)	174.79(5)	85.7(11)	94(3)
CH_2Cl	2.0789(11)	1.9375(2)	2.014(12)	3.3463(2)	177.82(6)	85.3(17)	95(3)
CHCl_2	2.083(1)	1.942(3)	2.009(4)	3.358(3)	177.2(6)	85.5(12)	94(2)
$\text{CH}_2\text{CH}_2\text{Cl}$	2.081(1)	1.925(6)	2.010(7)	3.324(5)	177.0(4)	85.7(15)	94(3)

^a Average values are given for multiple instances. Average deviations from the mean are given in square brackets. ^b Glowiak et al.³⁰ A = dihydrate. B = monohydrate.

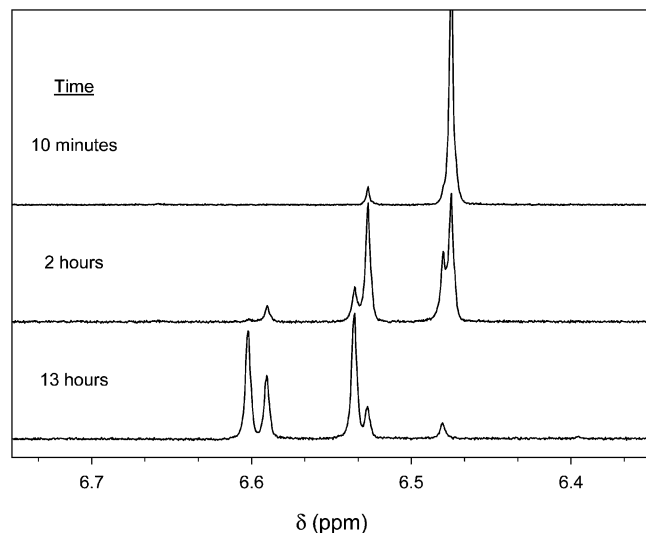


Figure 3. ^1H NMR spectra for Rh_3^+ ($\text{R} = \text{CHCl}_2$) during a water substitution experiment ($T = 313.5$ K; $[\text{Rh}_3^+] = 12$ mM). The signal at 6.475 ppm is from the triqua form of the trimer. Signals at 6.480 and 6.527 ppm (1:2), 6.534 and 6.590 ppm (2:1), and 6.602 ppm are due to the monosubstituted methanol trimer, disubstituted trimer, and trisubstituted trimer, respectively.

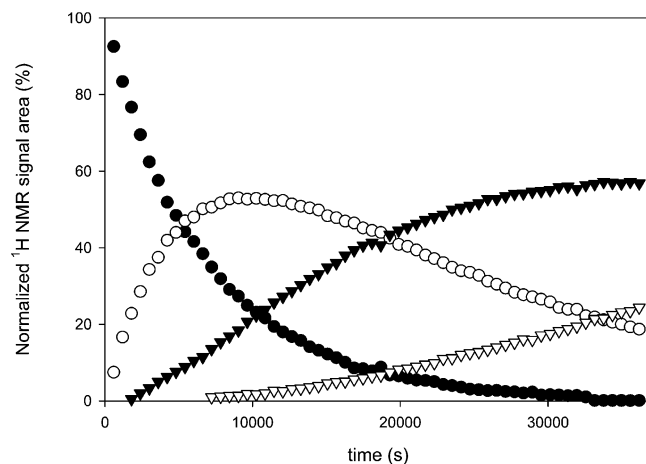


Figure 4. Variation of the ^1H NMR signal intensity for all four Rh_3^+ ($\text{R} = \text{CHCl}_2$) species as a function of time: the triqua trimer (●), the monomethanol-substituted trimer (○), the disubstituted trimer (▼), and the trisubstituted trimer (▽).

for all rhodium(III) trimers are reported in Table S1 in the Supporting Information.) Figure 4 shows the relative concentrations (in percent) of all four Rh_3^+ ($\text{R} = \text{CHCl}_2$) species in solution as a function of time. Because we are interested in only substitution of water at the triqua form of the trimer, very little data for subsequent substitutions were collected. Summarized in Table 3 are rate constants for $T = 298$ K

($k^{298\text{K}}$ estimated from ΔH^\ddagger and ΔS^\ddagger), activation parameters, and ^{103}Rh NMR chemical shifts for all five trimers. As the inductive ability of the R substituent increases, we see a decrease in the kinetic reactivity of the $\eta\text{-OH}_2$, a gradual increase in activation enthalpies, and a decrease in chemical shielding about the rhodium(III) nuclei.

Discussion

Even though the R substituents are located four bonds away from the isolated waters, the inductivity ability of these groups has a profound effect on the substitution rates. As the electron-withdrawing ability of the aliphatic group increases, the reaction rates decrease and span nearly 3 orders of magnitude ($k^{298\text{K}} = 10^{-2}$ – 10^{-5}), reflecting the following trend: $\text{R} = \text{CH}_2\text{CH}_3 > \text{CH}_3 > \text{CH}_2\text{CH}_2\text{Cl} > \text{CH}_2\text{Cl} > \text{CHCl}_2$. Often, the rates of substitution can be linked to the degree of covalency between the metal ions and the coordinated ligands. For Rh_3^+ , this amount of covalency is reflected, albeit roughly, in the crystallography data (Table 2). The Rh–OH₂ bond distances for the three complexes with the more electron-withdrawing groups ($\text{R} = \text{CH}_2\text{CH}_2\text{Cl}$, CH_2Cl , and CHCl_2) are shorter than the Rh–OH₂ bond lengths for the two trimers that have good σ donors ($\text{R} = \text{CH}_3$ and CH_2CH_3). However, the Rh–OH₂ bond distances for Rh_3^+ ($\text{R} = \text{CH}_2\text{CH}_2\text{Cl}$, CH_2Cl , and CHCl_2) all appear to be equal even though the inductive ability of each R substituent is considerably different. Thus, the $\eta\text{-OH}_2$ labilities are only crudely represented in bond distances. Also shown in Table 2 are O(H_2O)–Rh–O($\mu\text{-O}_2\text{CR}$) bond angles for all five trimers. Because these angles are all virtually identical (Table 2), steric effects likely play a minimal role in controlling the reaction rates within the series; hence, the difference in the reaction rates is purely inductive. These data indicate that σ donation from the six $\mu\text{-O}_2\text{CR}$ ligands, combined with electron donation from the central $\mu_3\text{-O}$, is the reason Rh_3^+ ($\text{R} = \text{CH}_3$) is 10^6 times more labile than $[\text{Rh}(\text{OH}_2)_6]^{3+}$, which is remarkable.

This trend in the reaction rates is also reflected in the activation parameters (Table 3). As the electron-withdrawing ability of the R group increases so too do the activation enthalpies ($\Delta H^\ddagger = 99$ – 115 kJ mol^{−1}) and, roughly, the entropies ($\Delta S^\ddagger = 48$ – 52 J mol^{−1} K^{−1}). For those Rh_3^+ ions with larger activation parameters [i.e., Rh_3^+ ($\text{R} = \text{CHCl}_2$); $\Delta H^\ddagger = 115$ kJ mol^{−1}, $\Delta S^\ddagger = 52$ J mol^{−1} K^{−1}], there is a greater degree of bond breaking vs bond formation during the formation of the activated complex. These results suggest that, as the inductive ability of the substituent increases, the

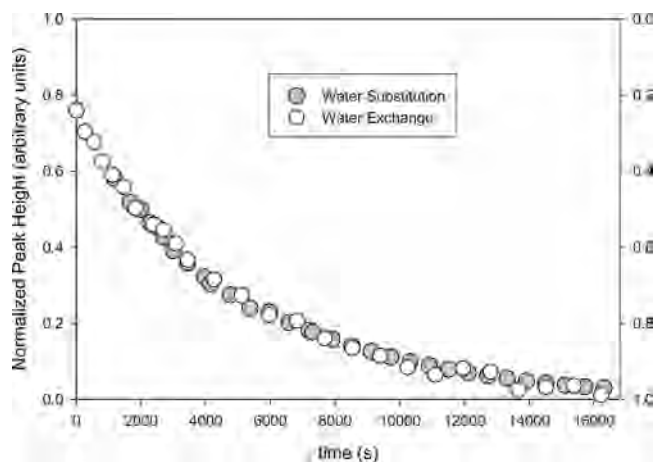


Figure 5. Kinetic data for water substitution and water exchange from Rh_3^+ ($\text{R} = \text{CH}_3$) at $T = 276.3 \text{ K}$ ($\pm 0.3 \text{ K}$). For the water substitution experiment, exponential decay of the ^1H NMR signal due to the triqua form of the trimer was followed as a function of time. Exponential growth of the ^{17}O NMR signal due to exchange of $\eta\text{-OH}_2$ with bulk $^{17}\text{OH}_2$ is shown with data inverted on the y axis (ordinate on the right).⁹ The rate constants are $2.03 (\pm 0.06) \times 10^{-4}$ and $2.04 (\pm 0.04) \times 10^{-4} \text{ s}^{-1}$ for water substitution and water exchange, respectively.

Table 3. Rates and Activation Parameters for Water Substitution by Methanol- d_4 from $[\text{Rh}_3(\mu_3\text{-O})(\mu\text{-O}_2\text{CR})_6(\text{OH}_2)_3]^+$ ($\text{R} = \text{CH}_2\text{CH}_3$, CH_3 , $\text{CH}_2\text{CH}_2\text{Cl}$, CH_2Cl , and CHCl_2)^a

Rh_3^+ ($\text{R} =$)	$k^{298\text{K}}$ (s^{-1})	ΔH^\ddagger (kJ mol^{-1})	ΔS^\ddagger ($\text{J mol}^{-1} \text{ K}^{-1}$)	^{103}Rh NMR chemical shifts (ppm)
CH_2CH_3	1.2×10^{-2}	$99(\pm 4)$	$50 (\pm 17)$	9406
CH_3	5.6×10^{-3}	$101(\pm 5)$	$51(\pm 20)$	9428
$\text{CH}_2\text{CH}_2\text{Cl}$	1.7×10^{-3}	$103(\pm 8)$	$48(\pm 30)$	9436
CH_2Cl	5.0×10^{-4}	$107(\pm 5)$	$50(\pm 17)$	9489
CHCl_2	2.3×10^{-5}	$115(\pm 3)$	$52(\pm 9)$	9620

^a The rates of water substitution at $T = 298 \text{ K}$ were estimated based on the activation parameters. Also tabulated are ^{103}Rh NMR chemical shift data for all five trimers [solution pH 1.9–2.2 (± 0.1); $T = 338.7 \text{ K}$].

mechanism of substitution gradually becomes slightly more dissociative in character. However, because the uncertainty for ΔH^\ddagger and ΔS^\ddagger is somewhat large for those compounds in which the temperature range was small, we cannot use the activation parameters to unequivocally distinguish reaction mechanisms among this family of compounds.

Assignment of a dissociative activation pathway is consistent with the I_d mechanism already established for water exchange from Rh_3^+ ($\text{R} = \text{CH}_3$; $\Delta V^\ddagger = +5.3 \text{ cm}^3 \text{ mol}^{-1}$),⁹ although these authors recognize that the use of Swaddle's semiempirical model³⁵ for activation volumes may not fully apply to larger clusters, such as these. Because there is little association with the incoming methanol molecule during the formation of the transition-state complex, the rates of water substitution are most likely good estimates of the exchange rates. In fact, the rate of water substitution by methanol- d_4 for Rh_3^+ ($\text{R} = \text{CH}_3$) is similar to the rate of exchange of bound and bulk waters for this molecule reported by Houston et al.⁹ (Figure 5; $T = 276.3 \text{ K}$). The rate constants are identical to within experimental error, indicating that the mechanism of exchange for Rh_3^+ ($\text{R} = \text{CH}_3$) may be more

(35) Swaddle, T. W. *Inorg. Chem.* **1983**, *22*, 2663–2665.

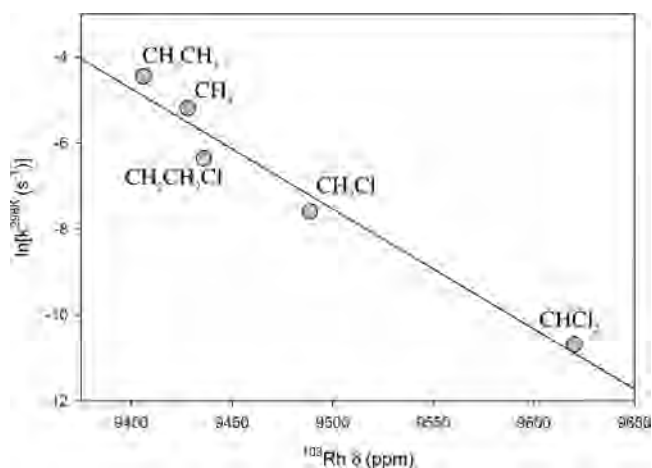


Figure 6. ^{103}Rh NMR chemical shifts ($T = 338.7 \text{ K}$) vs water substitution rates [$T = 298 \text{ K}$ (± 0.5)] for all five Rh_3^+ complexes ($R^2 = 0.964$; slope = -0.0279 , intercept = 257.84). The R substituents are denoted on the plot to identify each of the Rh_3^+ ions.

dissociative than indicated by the activation volume. Even so, these data suggest that the kinetic reactivity of $\eta\text{-OH}_2$ is greatly influenced by the inductive ability of $\mu\text{-O}_2\text{CR}$ and that the mechanism of substitution continues to have a considerable dissociative character.

Because the $\text{Rh}\text{-OH}_2$ bond distances do not vary consistently across the series, no firm conclusions can be drawn about the degree of covalency, and hence lability, of $\eta\text{-OH}_2$ from crystal data alone. The ^{103}Rh NMR chemical shifts, however, can provide some insight because chemical shifts reflect the degree of electron density around the nuclei. The chemical shifts for the five trimers span 214 ppm, in which the ^{103}Rh shielding decreases in the order of $\text{R} = \text{CH}_2\text{-CH}_3 > \text{CH}_3 > \text{CH}_2\text{CH}_2\text{Cl} > \text{CH}_2\text{Cl} > \text{CHCl}_2$. This trend in chemical shielding is the same trend observed for water substitution rates ($k^{298\text{K}}$; $\text{R} = \text{CH}_2\text{CH}_3 > \text{CH}_3 > \text{CH}_2\text{CH}_2\text{Cl} > \text{CH}_2\text{Cl} > \text{CHCl}_2$). Shown in Figure 6 are the ^{103}Rh NMR chemical shifts plotted against water substitution rates at 298 K ($R^2 = 0.964$). The small scatter may be due to slight differences in the sample temperature and solution viscosity, which are amplified here because of the enormous sensitivity of ^{103}Rh NMR chemical shifts, but these differences are small and could not possibly account for the 214 ppm span of ^{103}Rh NMR signals. Because ^{103}Rh NMR chemical shifts cover a wide range of frequencies ($\sim 12\,000 \text{ ppm}$), large variations in the chemical shifts reflect small electronic changes within the coordination sphere of the ^{103}Rh nuclei and thus can be used to investigate subtle electronic changes in the structure and subsequent reactivity at the metal centers.^{36–40} This correlation indicates that ^{103}Rh NMR chemical shifts could be used as a probe for estimating water exchange rates from other oxo-centered rhodium(III) trimers.

(36) von Philipsborn, W. *Chem. Soc. Rev.* **1999**, *28*, 95–105.

(37) Tedesco, V.; von Philipsborn, W. *Magn. Reson. Chem.* **1996**, *34*, 373–376.

(38) Koller, M.; von Philipsborn, W. *Organometallics* **1992**, *11*, 467–469.

(39) Tedesco, V.; von Philipsborn, W. *Organometallics* **1995**, *14*, 3600–3602.

(40) Graham, P. B.; Rausch, M. D.; Taeschler, K.; von Philipsborn, W. *Organometallics* **1991**, *10*, 3049–3052.

Conclusion

Substituent effects in four new oxo-centered rhodium(III) trimers, $[\text{Rh}_3(\mu_3\text{-O})(\mu\text{-O}_2\text{CR})_6(\text{OH}_2)_3]^+$ ($\text{R} = \text{CH}_2\text{CH}_3$, $\text{CH}_2\text{-CH}_2\text{Cl}$, CH_2Cl , and CHCl_2), and $[\text{Rh}_3(\mu_3\text{-O})(\mu\text{-O}_2\text{CCH}_3)_6(\text{OH}_2)_3]^+$ result in water substitution rates that span 3 orders of magnitude without changing the mechanistic pathway. The activation parameters consistently indicate a mechanism with considerable dissociative character for all five trimers; therefore, the rates of water substitution are most likely good estimates of the water exchange rates. By comparing ^{103}Rh NMR chemical shifts to water substitution rates, we provide a structure–reactivity correlation that allows one to predict water exchange from other oxo-centered rhodium(III) trimers from chemical shift data alone.

Acknowledgment. Support for this research was from American Chemical Society (Petroleum Research Fund 40412-AC2). The 500-MHz NMR was purchased using Grant OSTI 97-24412. The authors gratefully acknowledge three anonymous reviewers.

Supporting Information Available: Rate data for the five trimers at all experimental temperatures (Table S1), ^1H NMR spectra of all five rhodium(III) complexes (Figure S1), and CIF files and thermal ellipsoid plots for the four new compounds, including the 3-chloropropionate-bridged rhodium(II) dimer. This material is available free of charge via the Internet at <http://pubs.acs.org>.

IC060837G